16. Egerton, R. F. *Electron Energy Loss Spectroscopy in the Electron Microscope* (Plenum, New York, 1996).
17. Zhang, Z., Sigle, W. & Rühle, M. Atomic and electronic characterization of the *a*[100] dislocation core in $SrTiO_3$. *Phys. Rev. B* **66,** 094108 (2002).
18. Browning, N. D., Moltaji, H. O. & Buban, J. P. Investigation of three-dimensional grain-boundary structures in oxides through multiple-scattering analysis of spatially resolved electron-energy-loss spectra. *Phys. Rev. B* **58,** 8289–8300 (1998).
19. Yamada, H. & Miller, G. R. Point defects in reduced strontium titanate. *J. Solid State Chem.* **6,** 169–177 (1973).
20. Gong, W. *et al.* Oxygen-deficient $SrTiO_{3-x}$, x = 0.28, 0.17, 0.08. Crystal growth, crystal structures, magnetic, and transport properties. *J. Solid State Chem.* **90,** 320–330 (1991).
21. Abbate, M. *et al.* Soft-x-ray-absorption studies of the location of extra charges induced by substitution in controlled-valence materials. *Phys. Rev. B* **44,** 5419–5422 (1991).
22. Ohtomo, A., Muller, D. A., Grazul, J. L. & Hwang, H. Y. Epitaxial growth and electronic structure of $LaTiO_x$ films. *Appl. Phys. Lett.* **80,** 3922–3925 (2002).
23. Ohtomo, A., Muller, D. A., Grazul, J. L. & Hwang, H. Y. Artificial charge-modulation in atomic-scale perovskite titanate superlattices. *Nature* **419,** 378–380 (2002).
24. Howie, A. Image contrast and localized signal selection techniques. *J. Microsc.* **17,** 11–23 (1979).
25. Kirkland, E. J., Loane, R. F. & Silcox, J. Simulation of annular dark field STEM images using a modified multislice method. *Ultramicroscopy* **23,** 77–96 (1987).
26. Hillyard, S. E. & Silcox, J. Detector geometry, thermal diffuse scattering and strain effects in ADF STEM imaging. *Ultramicroscopy* **58,** 6–17 (1995).
27. Perovic, D. D., Rossow, C. J. & Howie, A. Imaging elastic strains in high-angle annular dark-field scanning-transmission electron microscopy. *Ultramicroscopy* **52,** 353–359 (1993).
28. Voyles, P. M., Muller, D. A. & Kirkland, E. J. Depth-dependent imaging of individual dopant atoms in silicon. *Microsc. Microanal.* **10,** 291–300 (2004).
29. Szot, K., Speier, W., Carius, R., Zastrow, U. & Beyer, W. Localized metallic conductivity and self-healing during thermal reduction of $SrTiO_3$. *Phys. Rev. Lett.* **88,** 075508 (2002).
30. Szot, K. & Speier, W. Surfaces of reduced and oxidized $SrTiO_3$ from atomic force microscopy. *Phys. Rev. B* **60,** 5909–5926 (1999).

Supplementary Information accompanies the paper on **www.nature.com/nature**.

Acknowledgements We acknowledge partial support from NEDO's International Joint Research Program. N.N. acknowledges partial support from QPEC, Graduate School of Engineering, University of Tokyo. D.A.M. and J.L.G. received partial support from the Cornell Center for Materials Research, a NSF materials research science and engineering centre.

Competing interests statement The authors declare that they have no competing financial interests.

Correspondence and requests for materials should be addressed to D.A.M. (davidm@ccmr.cornell.edu).

Vigorous exchange between the Indian and Atlantic oceans at the end of the past five glacial periods

Frank J. C. Peeters[1,2], Ruth Acheson[3], Geert-Jan A. Brummer[2], Wilhelmus P. M. de Ruijter[4], Ralph R. Schneider[5], Gerald M. Ganssen[1], Els Ufkes[1] & Dick Kroon[1]

[1]*Department of Paleoecology and Paleoclimatology, Faculty of Earth and Life Sciences, Vrije Universiteit, de Boelelaan 1085, 1081 HV, Amsterdam, The Netherlands*
[2]*Department of Marine Chemistry and Geology (MCG), Royal Netherlands Institute for Sea Research (NIOZ), PO Box 59, 1790 AB Den Burg, Texel, The Netherlands*
[3]*School of GeoSciences, The University of Edinburgh, Grant Institute, The King's Buildings, Edinburgh EH9 3JW, UK*
[4]*Faculty of Physics and Astronomy, Institute for Marine and Atmospheric Research Utrecht, Utrecht University, Princetonplein 5, 3584 CC Utrecht, The Netherlands*
[5]*Département de Géologie et Océanographie, UMR 5805 EPOC, CNRS/Université de Bordeaux I, 33405 Talence, France*

The magnitude of heat and salt transfer between the Indian and Atlantic oceans through 'Agulhas leakage' is considered important for balancing the global thermohaline circulation[1–3]. Increases or reductions of this leakage lead to strengthening or weakening of the Atlantic meridional overturning and associated variation of North Atlantic Deep Water formation[4–6]. Here we show that modern Agulhas waters, which migrate into the south Atlantic Ocean in the form of an Agulhas ring, contain a characteristic assemblage of planktic foraminifera. We use this assemblage as a modern analogue to investigate the Agulhas leakage history over the past 550,000 years from a sediment record in the Cape basin. Our reconstruction indicates that Indian–Atlantic water exchange was highly variable: enhanced during present and past interglacials and largely reduced during glacial intervals. Coherent variability of Agulhas leakage with northern summer insolation suggests a teleconnection to the monsoon system. The onset of increased Agulhas leakage during late glacial conditions took place when glacial ice volume was maximal, suggesting a crucial role for Agulhas leakage in glacial terminations, timing of interhemispheric climate change[7] and the resulting resumption of the Atlantic meridional overturning circulation[6].

The magnitude and intensity of the transport flux of heat and salt between the Indian and Atlantic oceans play a decisive role in global ocean circulation and the Atlantic meridional overturning circulation[1–6,8–11]. Surface and intermediate water transport from the Indian into the Atlantic Ocean takes place through the detachment of rings, eddies, and filaments from the Agulhas current and retroflection[2,10]. Whereas the modern hydrographic variability of the Agulhas system has been studied extensively[1–3,8–10], the palaeo-oceanography on orbital timescales (10^4–10^5 yr) is virtually uninvestigated, although some records have appeared[12,13]. Here we report new findings on the unique planktic foraminiferal signature of a modern Agulhas ring. We use this information as a modern analogue to disclose the late Pleistocene evolution of Agulhas transport into the South Atlantic using fossil planktic foraminifera.

Surface waters in the Cape basin may be derived from three different regions[2,9,10]: (1) the Indian Ocean's Agulhas current, (2) the South Atlantic current, north of the Sub-Tropical Convergence (STC), and (3) the subantarctic surface waters south of the STC. The MARE expeditions[14] examined a ~300-km-wide Agulhas ring called 'Astrid' (Fig. 1a), spawned from the Agulhas retroflection in January 2000 (ref. 15). Its faunal content was sampled by using depth-stratified plankton towing in the centre, near the boundary and the outside of the ring in March 2000, July/August 2000 and February 2001 (see Supplementary Information). These modern observations show that the ring is characterized by typical tropical–subtropical species[16,17] (Table 1). The most important are *Globigerinoides ruber*, *Globigerinoides sacculifer*, *Globigerinella siphonifera*, *Globigerinita glutinata*, *Orbulina universa*, *Globorotalia menardii* and *Globoquadrina hexagona* (Table 1, Methods). The modern distribution of living and seafloor fossil planktic foraminifera in the Indian and Atlantic oceans is discussed extensively elsewhere[16–18]. Identification of Agulhas fauna in ring Astrid agrees well with previous findings that the Agulhas current transports these species into the Cape basin. Faunal signatures can now be assigned to each of the Cape basin surface water masses. The Agulhas leakage water is traced by the Agulhas leakage fauna (ALF, see Methods), whereas water masses of the subpolar and polar zones are characterized by *Turborotalita quinqueloba* and *N. pachyderma* (sin.)[16–18] (Fig. 1b). The species *Globorotalia inflata* and *Neogloboquadrina pachyderma* (dex.) are mostly found in waters of the southern subtropical to subantarctic zones, while subtropical to transitional waters mainly north of the STC (that is, north of ~42° S) are reflected by *Globorotalia truncatulinoides*. Consequently, we will use the ratio of *G. truncatulinoides*/(*N. pachyderma* (dex.)+*G. inflata*+*G. truncatulinoides*) as a proxy for the distance of the STC relative to our sediment core sites in the southern Cape Basin.

The late Pleistocene history of Agulhas leakage is reconstructed using planktic foraminiferal assemblage data from two sediment cores located precisely beneath the 'Agulhas ring corridor' in the

southern Cape basin. The cores GeoB-3603-2 and MD96-2081 were spliced (see Methods) to form the 550-kyr-old Cape Basin record (CBR). Characteristic changes and events in the down-core oxygen isotope ratio of the benthic foraminifer *Cibicides wuellerstorfi* ($\delta^{18}O_{benthic}$) served as control points for the age model tuned to the standard orbital chronostratigraphy[19] (see Supplementary Information) (Fig. 2a). A foraminifera-independent proxy for sea surface temperature[20] (SST) is available for the upper part of the CBR (core GeoB-3603-2) from ketone unsaturation ratio ($U^{K'}_{37}$) measurements (Figs 2b, 3e–i). Preservation of the highly abundant planktic foraminifera in the CBR is very good (see Supplementary Information) and species diversity is high (thirty species), reflecting the convergence of several major water masses. Records of the ALF and species vital to the understanding of past variability in Agulhas leakage are shown in Fig. 2c–h.

The ($U^{K'}_{37}$) SST and ALF proxy records show strong glacial–interglacial variation. Enhanced Indian–Atlantic transport is observed during interglacial stages (Figs 2, 3). During glacial stages the relative contribution of ALF is low, indicating that Indian–Atlantic communication was reduced or may have temporarily ceased during MIS-12. The initiation of the late glacial SST rise precedes maximum ice volume, as indicated by the $\delta^{18}O_{benthic}$ proxy (Figs 2a, b and 3e–h), while late glacial initiation of enhanced Agulhas leakage starts when glacial ice volume is maximal (Fig. 3e–i). The ALF and SST rapidly increase during the first half of the glacial terminations V to I (Fig. 3e–i) and were maximal during the second half. During interglacial MIS-11, Agulhas leakage was persistent over a period of ~60,000 yr—that is, from 430–370 kyr ago.

Simultaneous occurrence of subantarctic species and increased Agulhas leakage during MIS-9 and MIS-8 (Fig. 2g,h) may point to a narrowing of the leakage passage. The northward shift of frontal zones, as reflected in the STC proxy (Fig. 3c) and by the higher relative abundance of subantarctic–Antarctic species (Fig. 2g,h), must have resulted in increased northward transport of cold wedges of subantarctic surface water during the formation of rings at the Agulhas retroflection[10,12]. Narrowing of the Agulhas corridor may alternatively explain the anomalous occurrences of subantarctic and Antarctic species in the southeast Atlantic[21,22]. Leakage reaches a maximum again during Termination II (Figs 2c and 3b,f). From this maximum, the leakage declined through the later part of MIS-5 and into the period MIS 4 to MIS 2. Establishment of modern values occurred during MIS 2 and Termination I into the Holocene. The

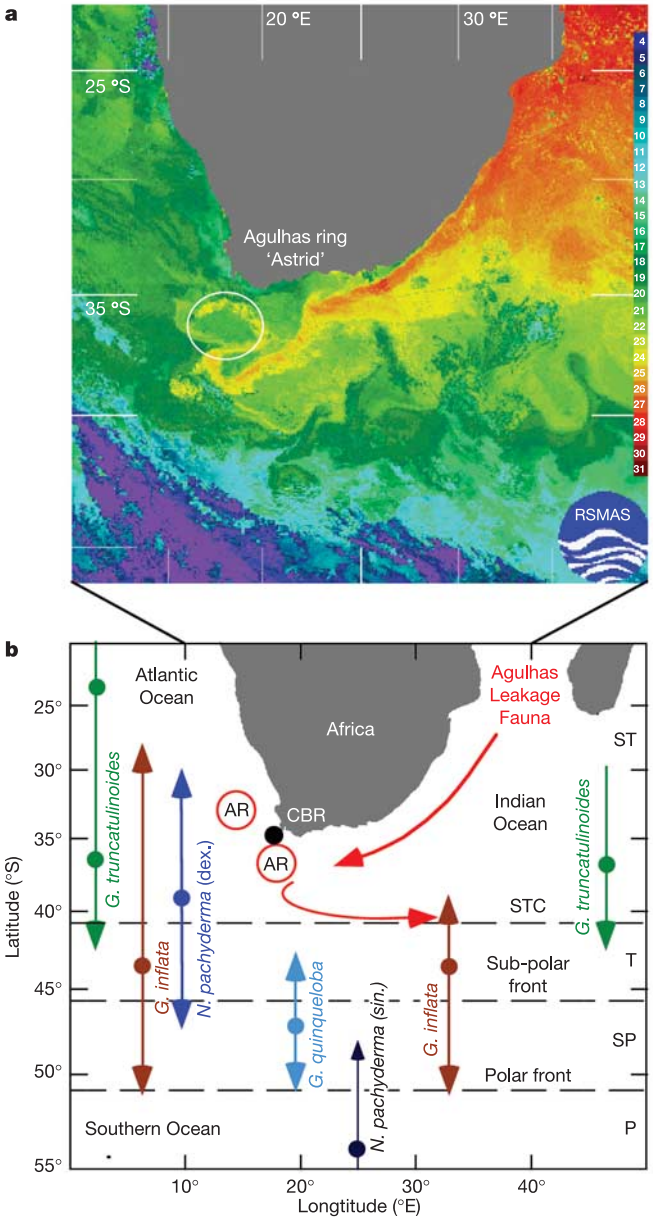

Figure 1 SST and latitudinal distribution of some planktic foraminifer species. **a**, Satellite image showing the SST of the Agulhas region in March 2000. The image clearly shows the extreme temperature contrast between the Agulhas current east of Africa and the southeast Atlantic. The circle indicates the position of Agulhas ring 'Astrid'[15], surrounded by a warm water filament, two months after spawning from the retroflection. The ring's faunal content was sampled by using depth-stratified plankton towing in the centre, the boundary and the outside of the ring in March 2000, July/August 2000 and February 2001 (see Supplementary Information). Image made available by the Rosenstiel School of Marine and Atmospheric Sciences, Miami, USA (http://www.rsmas.miami.edu/environment/imagery/). **b**, Schematic representation of the latitudinal distribution of some species of planktic foraminifera, as indicated by the arrows and position of frontal zones. The dots reflect the approximate position of the modern maximum relative abundance of the species[16–18]. Red arrows indicate transport direction of tropical and subtropical species, by the Agulhas current and retroflection. Circles labelled 'AR' show the pathway of Agulhas rings into the south Atlantic Ocean[10]. P, polar zone; SP, subpolar zone; T, transitional zone; ST, subtropical zone.

Table 1 **Living planktic foraminiferal assemblages off South Africa**

Species name	PCA-1	PCA-2	PCA-3	PCA-4	PCA-5
*Pulleniatina obliquiloculata**	**0.98**	0.00	0.09	0.06	0.04
*Globigerinita glutinata**	**0.96**	0.09	0.07	0.17	0.01
*Hastigerina pelagica**	**0.90**	0.12	0.01	0.03	−0.03
*Globorotalia menardii**	**0.86**	0.25	0.06	−0.09	0.10
Globigerinella calida	**0.70**	−0.05	**0.68**	0.00	0.07
*Globigerinoides sacculifer**	−0.05	**0.96**	−0.05	0.08	0.06
*Globigerinella siphonifera**	0.21	**0.92**	0.12	0.01	0.08
*Globigerinoides ruber**	0.33	**0.88**	−0.07	0.20	0.01
*Orbulina universa**	0.00	**0.86**	0.01	0.28	0.14
Neogloboquadrina dutertrei†	0.09	**0.54**	0.04	**0.75**	−0.11
Globorotalia hirsuta	−0.14	−0.04	**0.93**	−0.08	−0.01
Globorotalia truncatulinoides	0.29	−0.05	**0.91**	−0.05	0.10
Globorotalia inflata	0.09	0.25	**0.77**	**0.50**	0.06
Globigerina bulloides	0.29	0.29	0.15	**0.80**	−0.01
Neogloboquadrina pachyderma (dex.)	−0.13	−0.02	−0.11	**0.71**	0.22
Neogloboquadrina pachyderma (sin.)	−0.11	−0.19	−0.18	0.18	**0.67**
*Globoquadrina hexagona**	−0.04	−0.13	−0.15	−0.02	**− 0.60**
*Globorotalia scitula**	−0.11	−0.15	−0.07	0.02	**− 0.51**
Cumulative percentage of variance explained.	24	45	61	73	80

Numbers indicate the species' loading on Varimax-rotated principal components. Loadings greater than 0.50 or less than −0.50 are printed in boldface. Species marked with an asterisk are included in the Agulhas leakage fauna.
Interpretation of principal component assemblages. PCA-1, Agulhas leakage species with depth habitat 0–300 m; PCA-2, Agulhas leakage species with depth habitat 0–200 m (†*N. dutertrei* not included in reconstruction); PCA-3, Species inidicative for the subtropical to transitional zones with depth habitat 100–500 m; PCA-4, Species indicative for the transitional-subantarctic zones with depth habitat 0–200 m; PCA-5, Positive loading, that is, *N. pachyderma* (sin.), indicative for subantarctic to Antarctic zone. Negative loading indicates Agulhas leakage species with depth habitat 300–800 m.

faunal and SST record of the southern Benguela system[22] exhibit a similar pattern of late glacial increase of tropical species and SST over the last five glacial terminations, confirming the uptake of Agulhas water into the southeast Atlantic Ocean.

Variation in the ALF and STC proxy show a strong 100-kyr periodicity (Fig. 3b, c), indicating that the most dominant climate signal of Agulhas leakage variability is related to the periodic glacial–interglacial changes. The expansion of the Antarctic ice sheet, changes in the wind field[2], increased sea ice cover[23] and a northward position of the STC and frontal zones[13,24], may have contributed to the reduction of Agulhas leakage during glacial periods. A northward shift of the wind pattern results in a reduction of Agulhas leakage[2]. As the STC, reflecting the zero wind-curl line, approaches the tip of the continent, the southward-penetrating Agulhas effectively seals off the corridor through which Indian Ocean water leaks into the south Atlantic. Figure 3c shows that the STC reached its most northward position during mid-glacial conditions and not under late glacial conditions when continental ice volume was largest, effectively reducing the leakage into the South Atlantic.

The main orbital parameters affecting solar insolation and its distribution may have controlled the position of the STC and variations in Agulhas leakage. The dominant glacial–interglacial 100-kyr cycle is clearly present in most proxy records of the Cape basin (Figs 2b–f, 3a–c) and is most pronounced in the STC proxy (see Supplementary Information), showing most northward STC positions at minimum eccentricity (Fig. 3a,c). This implies that the amplitude modulation of precession by eccentricity (Fig. 3a) affects not only ice volume and tropical SST[20], but also the pattern of the wind field, the associated position of the STC and the variability of Agulhas leakage. Superimposed on the large-scale glacial–interglacial 100-kyr variability, the Agulhas leakage signal includes moderate tilt (41 kyr) and precessional (23 and 19 kyr) power (see Supplementary Information), implying both a 'low' and mid-high latitude forcing of the leakage. The relationship of the ALF to tilt is obviously related to the position of the frontal zones such as the STC and the associated shift in SSTs[25]. Comparison of the ALF with the solar insolation curves revealed that maxima in northern summer insolation and minima in precession are linked to maxima in ALF (Fig. 3a, b). We suggest that the increased strength of the monsoon

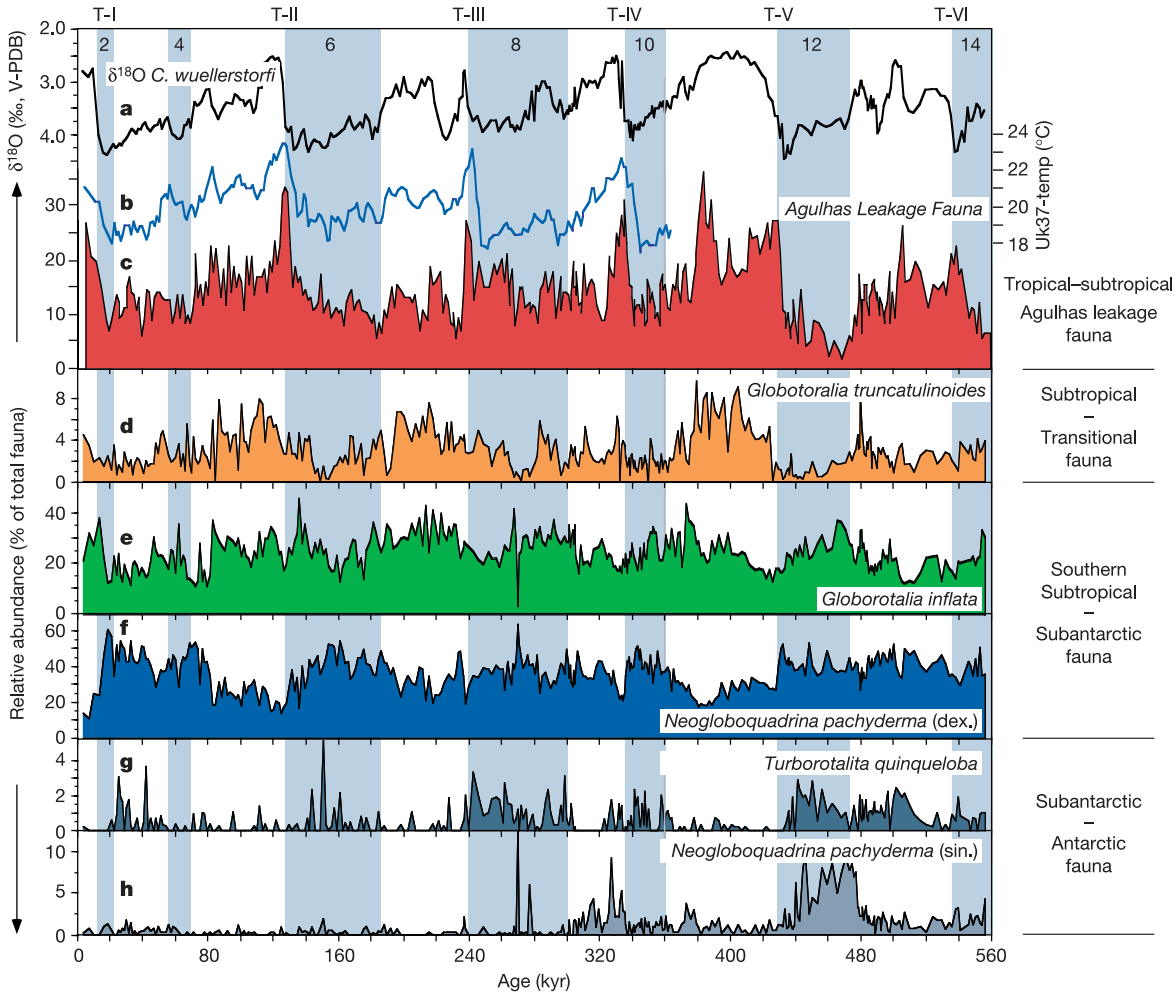

Figure 2 Late Pleistocene proxy records of the Cape Basin record. **a,** The oxygen isotope composition of the benthic foraminifer *Cibicides wuellerstorfi*, largely indicating global ice volume (V-PDB, Vienna Pee-Dee Belemnite standard). Even numbers at top refer to glacial Marine Isotopic Stages, T-I to T-VI refer to the major glacial terminations. **b,** The ($U^{K'}_{37}$) SST proxy for the upper part of the CBR (core GeoB-3603-2). **c,** The relative abundance of the Agulhas leakage fauna as a measure of Indian Ocean advection into the Atlantic. **d,** The relative abundance of *Globorotalia truncatulinoides*, indicative of subtropical-transitional waters. **e**, The relative abundance of *Globorotalia inflata* and **f**, *Neogloboquadrina pachyderma* (dex.) indicative of southern subtropical to subantarctic waters. **g**, The relative abundance of *Turborotalita quinqueloba*, reflecting subantarctic waters. **h**, The relative abundance of *Neogloboquadrina pachyderma* (sin.), indicative of Antarctic waters[16–18].

system promoted the equatorial transport of warm tropical waters feeding the Agulhas current and increased the Agulhas leakage. Based on an analysis of satellite altimetry data a relationship between the strength and variability of the Indian Ocean equatorial winds and the formation of rings from the Agulhas retroflection was recently proposed[26]. The signal propagates via a succession of Kelvin and Rossby waves that seems eventually to trigger the formation of rings. This implies that a stronger monsoon system results in an increase of the strength of this oceanic teleconnection between the equatorial and the southwest Indian Ocean, enhancing Agulhas ring formation and leakage.

Strongly guided by the African slope and Agulhas plateau, it is unlikely the Agulhas current would have deviated strongly from its present position during low sea level. A sediment record from beneath the Agulhas current to the south of and east of South Africa indicates that the glacial Agulhas current continued to flow and did not shift much laterally over the last 150,000 yr (ref. 27). The reduced glacial leakage is therefore probably caused by a further eastward retroflection of the Agulhas current, as has also been observed recently[28]. A northward shift of the STC and synchronous eastward forcing of the retroflection may have led to increased recirculation of tropical Agulhas water within the southern Indian Ocean. Such a mechanism would effectively transmit tropical signals to the southern Indian and Pacific oceans and might explain the increased glacial climate variability, with 'a northern hemispheric signature', in regions of the STC in the southern Indian and Pacific oceans[29].

The observation that modern Agulhas rings are characterized by an Indian Ocean faunal signature allows us to assess the variability of Indian–Atlantic water communication. The reconstructed history of Agulhas leakage provides important new data and insights into the processes and responses of climate-driven ocean circulation and places constraints on possible mechanisms of interhemispheric climate timing[7]. The late glacial rise in SST before the start of the

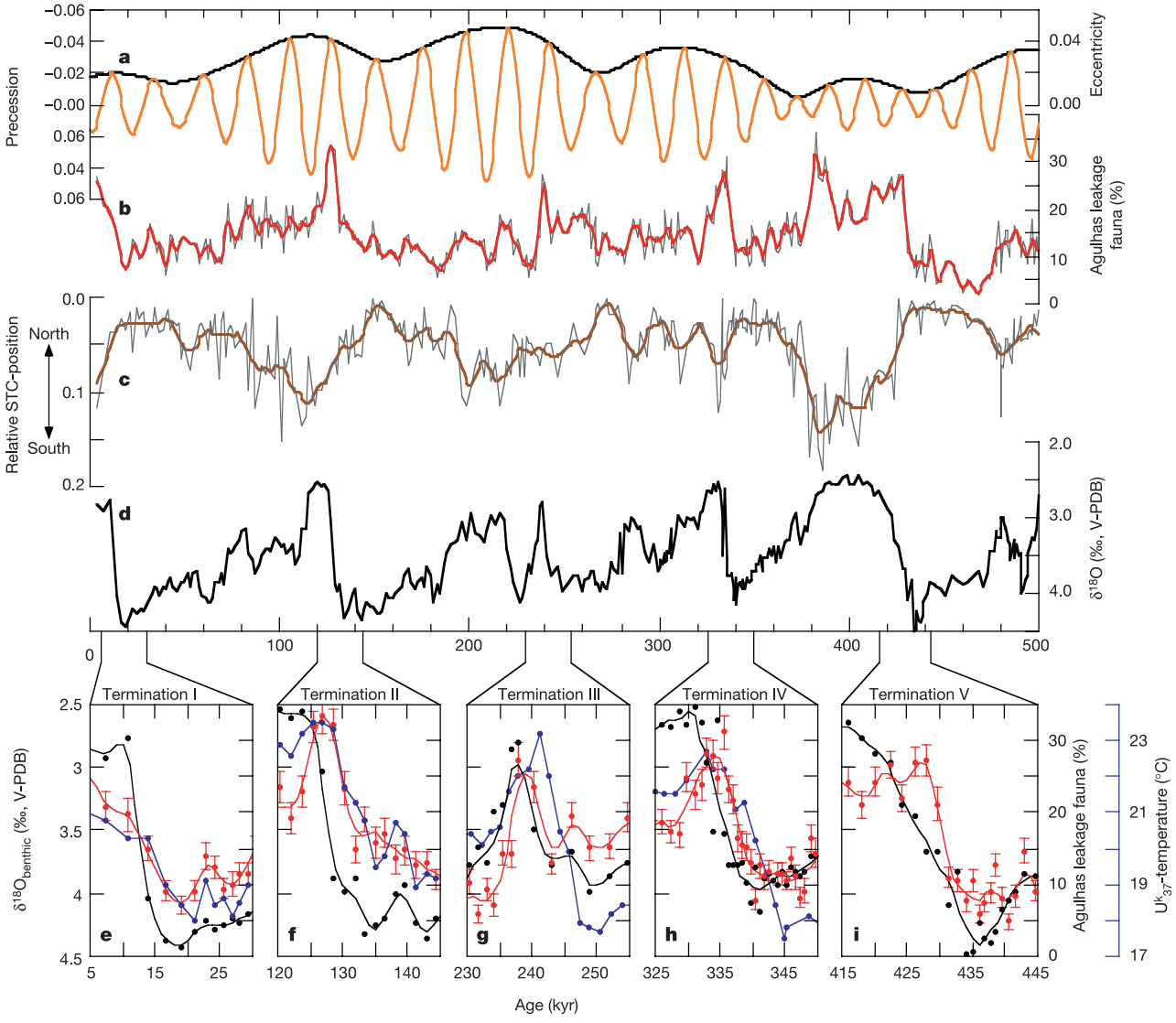

Figure 3 Late Pleistocene orbital variability and Cape basin proxy records during glacial terminations. **a**, Orbital eccentricity (black line) and precession (note inverted axis). **b**, The Agulhas leakage fauna. Periods of maximum Agulhas leakage appear to be related to minima in precession (maxima in northern summer insolation). **c**, The ratio of *G. truncatulinoides*/(*N. pachyderma* dex. + *G. inflata* + *G. truncatulinoides*) as a proxy for the distance of the STC relative to the position of the Cape basin record. High values indicate a southward position for the STC (note inverted axis). **d**, The $\delta^{18}O$ of *Cibicides wuellerstorfi*. **e–i**, The Cape basin proxy records of Agulhas leakage (red line), global ice volume (black line) and SST (blue line) during the major late Pleistocene glacial terminations I–V. Smoothed curves ($\delta^{18}O_{benthic}$ and ALF) represent seven-point smoothing of the 1-kyr sampled data. Original data indicated with dots. Error bars on the Agulhas leakage fauna specify one standard error of the mean.

major deglaciations and the onset of enhanced leakage when glacial ice volume is maximal underscore the potential role of Agulhas leakage in the resumption of Atlantic thermohaline circulation and North Atlantic Deep Water (NADW) formation[1–5,10]. This is confirmed by carbon and oxygen isotope records from cores located in the south Atlantic sector of the Southern Ocean[30]. Here, strong input of NADW into the Southern Ocean is observed during periods of maximum leakage. Our results support the conclusion of recent modelling results[6]—that abrupt resumption of the interglacial mode of the thermohaline circulation after glacial conditions is probably triggered by increased mass transport of Indian Ocean water into the Atlantic Ocean via the Agulhas system.

The faunal record also implies that the onset of a southward-moving STC, after reaching its most northward position during mid-glacial conditions, started well before the terminations and maxima in the leakage. Hence, the Indian–Atlantic connection via the Agulhas leakage should be considered an important marine amplifier for the 100-kyr cycle that dominates glacial–interglacial changes during the late Pleistocene. The flow of Indian Ocean water into the Atlantic is therefore indicative of changes in the global ocean-climate system and a precursor to re-establishment and maintenance of full interglacial conditions. □

Methods

The Agulhas leakage fauna

The Agulhas leakage fauna (ALF) includes all species loading greater than 0.85 on the first and second principal component axis (PCA) and species loading less than −0.50 on the fifth PCA (Table 1). The ALF thus includes the species: *Pulleniatina obliquiloculata*, *Globigerinita glutinata*, *Hastigerina pelagica*, *Globorotalia menardii*, *Globigerinoides sacculifer*, *Globigerinella siphonifera*, *Globigerinoides ruber*, *Orbulina universa*, *Globoquadrina hexagona* and *Globorotalia scitula*. This grouping appeared most consistent with the plankton tow observations when each station is studied one by one with respect to their position on the Agulhas ring studied (see also Supplementary Information). The ALF proxy used in this study is calculated as the sum of the relative abundance of the species listed above.

The Cape basin record

Two sediment cores, GeoB-3603-2 and MD96-2081 were used to form one time series. Both cores are located in very close proximity to each other, at similar depths within the southern Cape basin. Core GeoB-3603-2 was retrieved from 35° 08′ S to 17° 33′ E (2,840 m depth), while core IMAGES-II MD96-2081 is located at 35° 35′ S to 17° 41′ E (3,164 m depth). The cores are positioned on the upper slope, parallel to but south of Cape Canyon. Extensive analysis of the oxygen isotope data from both cores reveals that they overlap between 365 and 238 kyr. The joining point was taken at the peak of MIS 7.5. Samples in the overlapping section were removed to produce a single record which covers a continuous period of ~550 kyr. The upper portion of the spliced record uses samples from core GeoB-3603-2 and the lower section is core MD96-2081. Eighty-six of the samples from the bottom of core GeoB-3603-2 (708–1,133 cm below sea floor) are not included in the Cape basin record. The record described in this work relates to this spliced core and is referred to as the CBR. All characteristic glacial and interglacial stages of the Cape basin benthic $\delta^{18}O$ record were identified down to MIS 14 and tuned to the SPECMAP record, yielding an approximate age for the base of the record of ~550 kyr. Using this method MIS 5.5, 9 and 11 are isotopically the lightest. The glacial periods MIS 2, 6 and 10 have similarly high $\delta^{18}O$ values, whereas MIS 12 shows highest values during the late Pleistocene, indicating the most extreme glacial period of the time studied. More information on both cores can be found in the Supplementary Information.

Sampling resolution and faunal counts

Both cores were sampled every 5 cm, which produces an average temporal interval of ~1.5 kyr between two successive samples. Planktic foraminiferal counts were carried out on the >150-μm size fraction. To facilitate examination and counting, the fraction was divided using a microsplitter until approximately 400 specimens remained for counting. All faunal counts were based on at least 300 specimens per sample.

Spectral analysis

A Blackman–Tukey spectral cross-correlation between Northern Hemisphere summer insolation (21 June at 60° N) and (1) the Agulhas leakage fauna, and (2) the ratio of *Globorotalia truncatulinoides*/(*Neogloboquadrina pachyderma* (dex.)+*Globorotalia inflata*+*Globorotalia truncatulinoides*), was performed using the Analyseries software version 1.2 of ref. 31. The time interval between 4 and 500 kyr was analysed, using the 'compromise' option between resolution and confidence. This resulted in a number of lags of 149, or 30% of the series. The faunal abundance and oxygen isotope data were re-sampled every 1 kyr using the linear function integration method. The data were linearly detrended and normalized to unit variance before analysis. Bandwidth, 0.010.

Received 12 February; accepted 25 June 2004; doi:10.1038/nature02785.

1. Gordon, A. L. Communication between oceans. *Nature* **382,** 399–400 (1996).
2. de Ruijter, W. P. M. *et al.* Indian-Atlantic interocean exchange: Dynamics, estimation and impact. *J. Geophys. Res.* **104,** 20885–20910 (1999).
3. Gordon, A. L. The brawniest retroflection. *Nature* **421,** 904–905 (2003).
4. Weijer, W., de Ruijter, W. P. M. & Dijkstra, H. A. Stability of the Atlantic overturning circulation: Competition between Bering Strait freshwater flux and Agulhas heat and salt sources. *J. Phys. Oceanogr.* **31,** 2385–2402 (2001).
5. Weijer, W., De Ruijter, W. P. M., Sterl, A. & Drijfhout, S. S. Response of the Atlantic overturning circulation to South Atlantic sources of buoyancy. *Glob. Planet. Change* **34,** 293–311 (2002).
6. Knorr, G. & Lohmann, G. Southern Ocean origin for the resumption of Atlantic thermohaline circulation during deglaciation. *Nature* **424,** 532–536 (2003).
7. Wunsch, C. Greenland-Antarctic phase relations and millennial time-scale climate fluctuations in the Greenland ice-cores. *Quat. Sci. Rev.* **22,** 1631–1646 (2003).
8. Gordon, A. L., Weiss, R. F., Smethie, W. M. Jr & Warner, M. J. Thermocline and intermediate water communication between the South Atlantic and Indian oceans. *J. Geophys. Res.* **97,** 7223–7240 (1992).
9. Garzoli, S. L. & Gordon, A. L. Origins and variability of the Benguela Current. *J. Geophys. Res.* **101,** 897–906 (1996).
10. Lutjeharms, J. R. E. in *The South Atlantic: Present and Past Circulation* (eds Wefer, G., Berger, W. H., Siedler, G. & Webb, D. J.) 125–162 (Springer, Berlin/Heidelberg, 1996).
11. Macdonald, A. M. & Wunsch, C. An estimate of global ocean circulation and heat fluxes. *Nature* **382,** 436–439 (1996).
12. Rau, A. J. *et al.* A 450-kyr record of hydrological conditions on the western Agulhas Bank Slope, south of Africa. *Mar. Geol.* **180,** 183–201 (2002).
13. Flores, J.-A., Gersonde, R. & Sierro, F. J. Pleistocene fluctuations in the Agulhas Current Retroflection based on the calcareous plankton record. *Mar. Micropaleontol.* **37,** 1–22 (1999).
14. Lutjeharms, J. R. E. *et al.* MARE and ACSEX: new research programmes on the Agulhas Current System. *S. Afr. J. Sci.* **96** (2000).
15. van Aken, H. M. *et al.* Observations of a young Agulhas ring Astrid, during MARE in March 2000. *Deep-Sea Res. II* **50,** 167–195 (2003).
16. Bé, A. W. H. & Tolderlund, D. S. in *Micropaleontology of Oceans* (eds Funnell, B. M. & Riedel, W. R.) 105–149 (Cambridge Univ. Press, London, 1971).
17. Bé, A. W. H. & Hutson, W. H. Ecology of planktonic foraminifera and biogeographic patterns of life and fossil assemblages in the Indian ocean. *Micropaleontology* **23,** 369–414 (1977).
18. Niebler, H.-S. & Gersonde, R. A planktic foraminiferal transfer function for the southern South Atlantic Ocean. *Mar. Micropaleontol.* **34,** 213–234 (1998).
19. Imbrie, J. *et al.* in *Milankovitch and Climate I* (eds Berger, A. L., Imbrie, J., Hays, J. D., Kukla, J. & Salzman, J.) 269–305 (Reidel, Hingham, Massachusetts, 1984).
20. Schneider, R. R., Müller, P. J. & Acheson, R. in *Reconstructing Ocean History: A Window into the Future* (eds Abrantes, F. & Mix, A.) 35–55 (Kluwer Academic/Plenum, New York, 1999).
21. Ufkes, E., Jansen, J. H. F. & Schneider, R. R. Anomalous occurrences of *Neogloboquadrina pachyderma* (left) in a 420-ky upwelling record from Walvis Ridge (SE Atlantic). *Mar. Micropaleontol.* **40,** 23–42 (2000).
22. Chen, M.-T. *et al.* Late Quaternary sea-surface temperature variations in the southeast Atlantic: a planktic foraminifer faunal record of the past 600000 yr (IMAGES II MD962085). *Mar. Geol.* **180,** 163–181 (2002).
23. Kunz-Pirrung, M., Gersonde, R. & Hodell, D. A. Mid-Brunhes century-scale diatom sea surface temperature and sea ice records from the Atlantic sector of the Southern Ocean (ODP Leg 177, Sites 1093, 1094 and core PS2089–2). *Palaeogeogr. Palaeoclimatol. Palaeoecol.* **182,** 305–328 (2002).
24. Howard, W. R. & Prell, W. L. Late Quaternary surface circulation of the southern Indian Ocean and its relationship to orbital variations. *Paleoceanography* **7,** 79–117 (1992).
25. Sachs, J. P., Anderson, R. F. & Lehman, S. J. Glacial surface temperatures of the southeast Atlantic Ocean. *Science* **293,** 2077–2079 (2001).
26. Schouten, M. W., de Ruijter, W. P. M., van Leeuwen, P. J. & Dijkstra, H. A. An oceanic teleconnection between the equatorial and southern Indian Ocean. *Geophys. Res. Lett.* **29**(16), doi:101029/2001GL014542 (2002).
27. Winter, A. & Martin, K. Late Quaternary history of the Agulhas current. *Paleoceanography* **5,** 479–486 (1990).
28. de Ruijter, W. P. M. *et al.* Eddies and dipoles around South Madagascar: formation, pathways and large-scale impact. *Deep-Sea Res. I* **51,** 383–400 (2004).
29. Pahnke, K., Zahn, R., Elderfield, H. & Schulz, M. 340,000-year centennial-scale marine record of Southern Hemisphere climatic oscillation. *Science* **301,** 948–952 (2003).
30. Hodell, D. A., Charles, C. & Ninnemann, U. S. Comparison of interglacial stages in the South Atlantic sector of the southern ocean for the past 450 kyr: implications for Marine Isotope Stage (MIS) 11. *Glob. Planet. Change* **24,** 7–26 (2000).
31. Paillard, D., Labeyrie, L. & Yiou, P. Macintosh program performs time-series analysis. *Eos Trans. AGU* **77,** 379 (1996).

Supplementary Information accompanies the paper on **www.nature.com/nature**.

Acknowledgements The MARE/CLIVARNET project was sponsored by two NWO grants (bilateral cooperation programme NWO-DFG). R.A. acknowledges funding from a NERC grant. R.S. is grateful to the German Science Foundation (DFG) and the IMAGES programme for sponsoring core retrieval and analytical work. We thank M. Segl and P. Mueller for measuring isotopes and alkenones, respectively. We thank the captain and crew of R/V *Pelagia* and R/V *Agulhas* as well as the Royal NIOZ technicians. We thank all MARE team members for discussion. This is a publication of the Netherlands Research School of Sedimentary Geology (NSG).

Competing interests statement The authors declare that they have no competing financial interests.

Correspondence and requests for materials should be addressed to F.P. (frank.peeters@falw.vu.nl).